Dalton Transactions

UV-Vis spectrophotometric determination of rare earth elements (REE) speciation at near-neutral to alkaline pH. Part II: hydrolysis of Er from 25 to 75 °C

Journal:	*Dalton Transactions*
Manuscript ID	DT-ART-10-2024-003037.R1
Article Type:	Paper
Date Submitted by the Author:	17-Feb-2025
Complete List of Authors:	Han, Hannah Juan; New Mexico Institute of Mining and Technology, Geology and Mining Resources Gysi, Alexander; New Mexico Institute of Mining and Technology, Earth and Environmental Science; New Mexico Bureau of Geology & Mineral Resources, New Mexico Institute of Mining and Technology

UV-Vis spectrophotometric determination of rare earth elements (REE) speciation at near-neutral to alkaline pH. Part II: hydrolysis of Er from 25 to 75 °C

Hannah Juan Han[1], Alexander Gysi[1,2]*

[1]New Mexico Bureau of Geology and Mineral Resources, New Mexico Institute of Mining and Technology, 801 Leroy Place, Socorro, NM 87801, USA

[2]Department of Earth and Environmental Science, New Mexico Institute of Mining and Technology, 801 Leroy Place, Socorro, NM 87801, USA

* Corresponding authors: alexander.gysi@nmt.edu

To be submitted to Dalton Transaction

Revision 1

KEYWORDS: *Rare earth elements, hydrolysis, UV-Vis spectrophotometry, meta-cresol purple, pH, Erbium*

Abstract

Aqueous speciation of rare earth elements (REE) controls their mobilization, fractionation, and enrichment in the natural waters. Geochemical modeling of their speciation is key to improve our understanding of the formation of economic mineral deposits, for developing mineral separation and mine tailing recovery technologies, and for characterizing the geochemistry of thermal water. However, our ability to predict the fate of REE in a wide pH and temperature range is limited by the scarcity of thermodynamic data for the REE hydroxyl complexes. In Part I of this study[1], the optical properties of *m*-cresol purple (*m*CP) were determined using UV-Vis spectrophotometry between 25 and 75 ℃ in order to develop a method for deriving the hydrolysis constants of erbium (Er). Here, UV-Vis spectrophotometry experiments were conducted as a function of temperature between 35 and 75 ℃ to determine the hydrolysis of Er in near-neutral to alkaline solutions using *m*CP as an *in situ* pH color indicator. The experiments were conducted with Er concentrations from 0 to ~0.253 mmol/kg in low ionic strength solutions (≤ 0.001 mol/kg). The average OH^- ligand number coordinated to Er^{3+} increases from 1.0 to 2.7 at 35 ℃ and from 1.5 to 3.2 at 75 ℃ over a pH range from 6.3 to 9.0. The measured speciation shows an increased predominance of $Er(OH)_3^0$ over the $Er(OH)^{2+}$ and $Er(OH)_2^+$ species with increased temperature. The logarithmic values of Er hydrolysis constants ($\log^*\beta_n^\circ$, n =1 to 3) were derived for the reaction $Er^{3+} + nH_2O = Er(OH)_n^{3-n} + nH^+$ at each temperature of 35, 50, and 75 ℃: $\log^*\beta_1^\circ$ of −7.02 ± 0.09, −6.19 ± 0.06, −5.43 ± 0.16; $\log^*\beta_2^\circ$ of −14.39 ± 0.15, −13.98 ± 0.01, and −13.45 ± 0.24; $\log^*\beta_3^\circ$ of −22.85 ± 0.15, −21.79 ± 0.14, and −20.32 ± 0.09. These equilibrium constants were fitted to a function to predict the hydrolysis constants of Er between 25 and 75 ℃, and show a systematic increase in the stability of REE hydroxyl complexes with higher ligand numbers with increased temperature.

1. Introduction

The aqueous speciation of rare earth elements (REE) controls their mobilization and fractionation during water-rock interaction and ore-forming processes.[2–4] Important REE aqueous complexes known to potentially mobilize the REE include chloride, fluoride, sulfate, carbonate, and hydroxyl complexes. Numerous experimental studies[5–7] have focused on the stability of most of these species at elevated temperature (>100 °C). In contrast, the behavior of REE hydroxyl complexes as a function of temperature is largely unknown due to a paucity of experimental data beyond 25 °C. This is in part due to a need to develop accurate *in situ* pH measurement techniques that can be used in hydrothermal aqueous solutions.

Potentiometry and UV-Vis spectrophotometry experiments have been considered for *in situ* pH measurements and determination of REE hydrolysis above room temperature. A few studies have investigated REE hydrolysis constants using potentiometry at temperatures between 30 and 70 °C and different ionic strengths ranging from 0.02 to 4 mol/L.[8–12] UV-Vis spectrophotometric experiments are generally absent at temperatures above 25 °C. The study by Hernández-García *et al.*[13] is the only UV-Vis study to date presenting experiments conducted at 30 °C for the first hydrolysis constant of Ho from pH 3 to 10. In Part I of this study, Han and Gysi[1] determined the optical properties for the pH color indicator *m*-cresol purple (*m*CP) up to 75 °C, which was used to determine *in situ* pH and the hydrolysis constants of Er at 25 °C. This method was applied previously for the REE hydrolysis at 25 °C, albeit without the updated *m*CP properties derived recently.[1,9,14,15]

Previous assessment of the speciation of REE[16–19] indicates an increase in the stability of hydroxyl complexes as function of temperature and pH. At temperature < 100 °C, Klungness and Byrne[9] reports the first hydrolysis constants for the formation of $REE(OH)^{2+}$ for all of the REE between 25 to 55 °C in solutions with 0.7 mol/L $NaClO_4$. İçhedef *et al.*[20] determined the

first to third hydrolysis constants of La and Sm for the formation of $REE(OH)^{2+}$, $REE(OH)_2^{+}$, and $REE(OH)_3^0$ from 25 to 45 °C in solutions with 0.1 mol/L KCl. Rodenas and Liberman[8] determined the first and second hydrolysis constants of Gd at temperatures up to 70 °C in solutions with 0.01 mol/L NaOH and $Gd(NO_3)_2$. Wood *et al.*[21] determined the first and third hydrolysis constants of Nd from 30 to 290 °C in 0.03 mol/kg NaTr solutions. A recent review by Jordan *et al.*[22] recommends that the $REE(OH)_4^-$ is discarded because it has not been determined to be stable at 25 °C even at high pH up to 13. Most of these studies above have been conducted at relatively high ionic strength. In addition, the properties of the heavy REE (Tb to Lu) hydroxyl complexes have not been well established in comparison to the light REE (La to Gd) at temperatures above 25 °C. Therefore, there is a need to accurately investigate the hydrolysis of REE to derive their equilibrium constants, especially for the heavy REE over a wider pH and temperature range to model their stability in natural waters.

In this study, we conducted a series of UV-Vis experiments to investigate the hydrolysis of Er at near-neutral to alkaline pH at a temperature up to 75 °C and an ionic strength of ≤ 0.001 mol/kg. The hydrolysis constants derived for the $Er(OH)^{2+}$, $Er(OH)_2^{+}$, and $Er(OH)_3^0$ species are compared with previous literature values, which allows fitting the experimental data and derive the Er hydrolysis constants ($^*\beta_n^\circ$, n = 1 to 3) between 25 and 75 °C. The new data are implemented in the MINES thermodynamic database[23] and permit simulating Er speciation using the geochemical modeling program GEM-Selektor[24,25]. The UV-Vis/*m*CP methods presented here yields a promising approach for understanding the stability of other REE hydroxyl complexes with pH and temperature, their coordination chemistry, and stability of different species in natural waters.

2. Materials and Methods

2.1. Materials

The experimental Er-bearing *m*CP-NaOH solutions were prepared from the stock solutions to achieve final concentrations of 0.030 mmol/kg *m*CP, 0.445 mmol/kg NaOH, and varying $ErCl_3$ concentrations of ranging from 0 to ~0.253 mmol/kg. The 0.15 mmol/kg *m*CP stock solution was prepared by dissolving pure *m*CP powder (Acros Organics, indicator grade) in Milli-Q water (18.2 MΩ·cm). The 0.005 mol/kg NaOH stock solution was prepared using a trace metal grade NaOH (Inorganic Ventures, 0. 9968 ± 0.001 M) diluted with Milli-Q water. The $ErCl_3$ stock solution was prepared by dissolving $ErCl_3 \cdot nH_2O$ (Sigma-Aldrich, ≥ 99.9 % purity) in Milli-Q water. The pH of the solutions ranges from ~6.3 to 9.5, which is controlled by the initial amount of NaOH and the amount of $ErCl_3$ added. The latter lowers the pH due to de-protonation associated to the hydrolysis of Er. All the experimental solutions were prepared daily with CO_2-degassed and ion exchange column purified Milli-Q water to minimize any interference from $CO_2(g)$ in solution.

2.2. UV-Vis experiments

The UV-Vis spectrophotometric experiments were carried out using *m*CP to measure *in situ* pH and the hydrolysis of Er at temperatures of 35, 50, and 75 °C in low ionic strength solutions (≤ 0.001 mol/kg). The UV-Vis/*m*CP method is based on the experiments by Han and Gysi[13] and using the reported *m*CP optical properties and dissociation constants. The experimental solutions with varying initial Er concentrations (0 to ~0.253 mmol/kg) and pH values from ~6.3 to 9.5 (Table S1) were placed in sealed 1 cm quartz cuvettes for UV-Vis spectrophotometry analysis. The temperature was controlled and monitored using a Peltier cell sample holder accessory with probes to determine temperature within ± 0.1 °C.

UV-Vis absorbance spectra were measured in each experimental solution from 350 to 750 nm using an Agilent Cary 5000 dual-beam spectrophotometer with 2.0 nm slit bandwidth. The wavelength accuracy and precision of the instrument were checked and calibrated using the deuterium arc lamp at 486 nm and 656.1 nm. Absorbance spectra of *m*CP were measured at each temperature in at least four replicate series covering the pH range of ~6.3 to 9.5 for each isotherm. The absorbance intensities of deprotonated and protonated forms of *m*CP were collected at their maximum absorbance wavelengths 578 nm and 434 to 428 nm, respectively. The shift of protonated species from 434 to 428 nm with temperature in the spectra is consistent with the experimental observation of mCP in 0.1 mmol/L HCl solution by Han and Gysi[1]. The Er-bearing *m*CP-NaOH solutions with the highest Er concentrations (~0.253 mmol/kg) display a transparent yellow color controlled by the protonated form of the *m*CP chromophore.

2.3. Potentiometric measurements

pH analysis was conducted at 35−75 °C using a Metrohm unitrode (serial number 6.0260.010) with a built-in Pt1000 temperature sensor and a Metrohm 913 pH meter. The electrode was calibrated using Fisher Scientific commercial buffer solutions (pH of 4, 7, and 10; accuracy of ± 0.01 pH units at 25 °C) with known pH as a function of temperature at each isothermo. The temperature of the samples and buffer solutions was kept constant ± 0.5 °C by immersing the solution vials into a water bath.

2.4. Erbium analysis

The Er concentration was measured in the $ErCl_3$ stock solutions using an Agilent 5900 inductively coupled plasma optical emission spectrometry (ICP-OES) instrument at the Analytical Chemistry Laboratory in the New Mexico Bureau of Geology and Mineral

Resources, New Mexico Institute of Mining and Technology. A trace metal grade 1000 ppm Indium stock solution provided from Inorganic Ventures was diluted with 2% HNO_3 to 10 ppm as an internal standard for drift correction in the ICP-OES measurements. A series of Er analytical calibration standards in a concentration ranging from 25 to 250 ppb were prepared from a 10 ppm multi-REE stock standard (Inorganic Ventures, NIST traceable standard) diluted with a 2% HNO_3 (Fisher Scientific, trace metal grade) blank matrix solution. The analytical precision in the diluted 176 ppb $ErCl_3$ stock solution is better than 3%. The detection limit for the ICP-OES run of Er was determined to be 1 ppb using repeated analysis of the procedural blank (5σ).

3. Data treatment

3.1. *In situ* pH determination using *m*CP

The pH values in the Er-bearing *m*CP-NaOH solutions depend on the hydrolysis reaction for $Er^{3+}$and release of H^+ according to:

$$Er^{3+} + nH_2O \leftrightarrow Er(OH)_n^{3-n} + nH^+ \quad \text{(R1)}$$

Addition of varying initial concentrations of $ErCl_3$ to the *m*CP-NaOH solutions drives the Er hydrolysis reaction to the right and produces protons with a corresponding decrease in pH. In turn, the *m*CP dissociation reaction shifts to the left side and results in an increased stability of the protonated species:

$$HI^- \leftrightarrow I^{2-} + H^+ \quad \text{(R2)}$$

where HI^- and I^{2-} represent the protonated and deprotonated forms of *m*CP, respectively. The UV-Vis spectra absorbance intensity of the protonated HI^- species therefore increases accompanied by a decrease in the absorbance intensity of the deprotonated I^{2-} species. Solution pH is determined *in situ* based on the properties of *m*CP and the measured absorbance of HI^- at 434 to 428 nm and I^{2-} at 578 nm using the following equation:

$$\mathrm{pH_T} = -\log e_2 K^o_{\mathrm{mCP,T}} + \log\left(\frac{R-e_1}{1-R\frac{e_3}{e_2}}\right) \quad (1)$$

where $K^o_{\mathrm{mCP,T}}$ is the dissociation constant of *m*CP at infinite dilution and temperature T (in °C); R is the absorbance intensity ratio of I^{2-} and HI^- (defined by Abs_{I2-}/Abs_{HI-}) at their maximum absorbance wavelengths; e_1 to e_3 are molar absorbance coefficients of *m*CP. The temperature dependent properties of *m*CP are taken from Part I of this study derived in Han and Gysi[1].

3.2. Calculation of the average OH^- ligand number and derivation of the Er hydrolysis constants

The average number of OH^- coordinated to Er^{3+} (average ligand number, $\vec{n}$) in the Er-bearing *m*CP-NaOH experimental solutions can be calculated from the pH values determined from the UV-Vis/*m*CP method (R1). The average ligand number reflects the OH^- coordinated to Er^{3+} by averaging each contributing hydroxyl species according to,

$$\vec{n} = \frac{m_{\mathrm{OH^-}} - m'_{\mathrm{OH^-}}}{m_{\mathrm{Er}}} = \frac{\sum n m_{\mathrm{Er(OH)_n^{3-n}}}}{m_{\mathrm{Er}}} \quad (2)$$

where m_{OH^-} and m'_{OH^-} are the amount of OH^- ligand in the Er-absent and Er-bearing *m*CP-NaOH solutions, respectively. Both values of these two terms are related to the pH

measurements by using the UV-Vis/*m*CP method. $\sum nm_{\mathrm{Er(OH)_n^{3-n}}}$ is retrieved from the difference of OH^- amount between the Er-absent and Er-bearing *m*CP-NaOH solutions; m_{Er} is the molality of total dissolved Er added to the experiment.

The cumulative hydrolysis constants at infinite dilution ($\log{}^*\beta_n^\circ$) to form $Er(OH)^{2+}$, $Er(OH)_2^+$, and $Er(OH)_3^0$ (R1, *n*=1 to 3) were derived from 35 to 75 °C using the calculated average ligand number and the measured pH of the solutions according to:

$$ {}^*\beta_n^\circ = \frac{m_{\mathrm{Er(OH)_n^{3-n}}} m_{\mathrm{H^{+n}}}}{m_{\mathrm{Er^{3+}}}} \cdot \frac{\gamma_{\mathrm{Er(OH)_n^{3-n}}} \gamma_{\mathrm{H^{+n}}}}{\gamma_{\mathrm{Er^{3+}}}} \quad (3) $$

where m_{H^+}, $m_{Er^{3+}}$, and $m_{Er(OH)_n^{3-n}}$ are the molalities, and γ_{H^+}, $\gamma_{Er^{3+}}$, and $\gamma_{Er(OH)_n^{3-n}}$ are the activity coefficients of the respective species. Since the ionic strength is ≤ 0.001 mol/kg, the activity coefficient in solutions were set to unity. The cumulative hydrolysis constants of Er can be calculated by combining eqn. (2) to (3) according to,

$$ \vec{n} = \frac{(1-\vec{n})\times{}^*\beta_1^o}{\mathrm{m_{H^+}}} + \frac{(2-\vec{n})\times{}^*\beta_2^o}{\mathrm{m_{H^+}}^2} + \frac{(3-\vec{n})\times{}^*\beta_3^o}{\mathrm{m_{H^+}}^3} \quad (4) $$

The hydrolysis constants of Er are retrieved by solving a 9×5 matrix by linear regression of the normal equation (P=inv(X'×X)×(X'×Y)) using Matlab (Version R2023a). The uncertainty associated with each of the hydrolysis constants was determined for each isotherm by calculating the standard deviation of the mean of a repeated series (4−6, Table S1) of experiments covering a pH range from 6.3 to 9.0.

4. Results and discussion

4.1. UV-Vis absorbance in Er-bearing solutions between 35 and 75 °C

The absorbance spectra of Er-absent and Er-bearing *m*CP-NaOH solutions are shown in Fig. 1 as a function of temperature with the experimental data listed in Table S1. For the Er-absent *m*CP-NaOH solutions at 35 °C, a strong absorbance peak is observed at 578 nm for the deprotonated I^{2-} form of *m*CP with a broad valley for the protonated HI^{-} species at 434 nm. An increase in temperature to 50 and 75 °C results in a slight UV-Vis spectra blue shift from 434 to 428 nm and a decrease of the absorbance intensities of both the I^{2-} and HI^{-} species, due to the pi-stacking of the *m*CP molecules.[26,27] These results are in agreement with the UV-Vis spectra observed in the *m*CP of 0.1 mmol/L HCl and 0.01 mol/L NaOH solutions at temperatures of 35−75 °C by Han and Gysi[1].

At 35 °C, addition of 0 to ~0.253 mmol/kg $ErCl_3$ to the *m*CP-NaOH solutions results in a gradual decrease of the UV-Vis absorbance intensity of the I^{2-} form of *m*CP and corresponding increase of the absorbance spectra of the HI^{-} species at each investigated temperature (Fig. 1). The HI^{-} species starts to form a strong peak after adding Er concentrations above 0.114 mmol/kg. An isosbestic point for the I^{2-} and HI^{-} species also appears at a wavelength 482 nm in the spectra, suggesting the concentration of *m*CP remains constant at 35 °C in these Er-absent and Er-bearing *m*CP-NaOH solutions. Therefore, there is no complexes formed between *m*CP and Er^{3+}.[28] An increase in temperature causes a blue shift for the well-defined isosbestic point of I^{2-} and HI^{-} species at wavelengths from 486 to 482 nm, which is consistent with the study by Liu *et al.*[29].

The *m*CP absorbance intensity ratio (R) of the I^{2-} to the HI^{-} species (defined by Abs_{I2-}/Abs_{HI-}) decreases with increased Er concentrations at all experimental temperatures (Fig. 2). At Er concentrations of 0.120 mmol/kg, the R value decreases more considerably and then

reaches a close to constant value above 0.151 mmol/kg Er. A shift to lower *R* values is observed with increased temperature from 35 to 75 °C due to an overall decrease in the absorbance intensity of the deprotonated I^{2-} species and concomitant increase in the absorbance intensity of the protonated HI^{-} species. Han and Gysi[1] report that the *m*CP optical properties e_1 and e_3/e_2 increase from 0.005 to 0.01 and 0.06 to 0.07 as the temperature increases from 35 to 75 °C. This suggests a narrowing range of *R* values to determine the pH of solution by using the UV-Vis/*m*CP method at high temperature (eqn (1)). Hence, there is a decrease in the sensitivity of the UV-Vis/*m*CP method for pH measurements at increased temperature.

4.2. Comparison to pH measured using the potentiometric method

Fig. 3 shows a comparison between pH values determined from the UV-Vis/*m*CP method versus values determined from potentiometric pH measurements. Overall, there is a close agreement between both methods at pH values between 7.5 and 9−9.5 and *R* values > 0.25. Depending on temperature, pH differences are generally within or better than 2.5 % or 0.25 pH units (Fig. 3D-F). In contrast, at pH <7.5 or for *R* values < 0.25, the pH differences can reach up to 6.3−7.5 % or ~0.4 pH units. These differences are partly due to a few shortcomings of each method. The potentiometric method displays some pH variations when using the electrodes in an open beaker due to possible $CO_2(g)$ contamination as well as the need for a longer stabilization time. The limitation of the UV-Vis/*m*CP method is the study of hydrolysis in a pH range only from ~6.3 to 9−9.5 in accordance with the *R* versus total Er concentrations (Fig. 2) with a decreased sensitivity in the lower pH range. Nevertheless, the overall systematic trends observed in the *R* versus pH data derived from the UV-Vis/*m*CP method (Fig. 3) indicates that it is a robust method for *in situ* pH determination at pH between ~ 6.3 and 9, and

has the advantage of shorter stabilization times and a lack of interference with atmospheric CO_2(g) in the closed quartz cuvette.

4.3. Average OH^- ligand number

The average number of OH^- ligands coordinated to Er^{3+} in the Er-bearing *m*CP-NaOH solutions is calculated from pH (eqn (2)). The calculated average ligand numbers are listed in Table S1 and shown in Fig. 4. Polynomial fits and their 95 % confidence and prediction interval and their regression coefficients (RSME and R^2) are listed in Table 1. At 35 °C (Fig. 4A), the average ligand number is ~ 1.0 at near-neutral pH and increases to ~ 2.7 at alkaline pH. These results suggest that $Er(OH)^{2+}$ is predominant at pH < 7.5 and shifts to the $Er(OH)_2^+$ and $Er(OH)_3^0$ species at pH between 7.5−9. In the experiments conducted at 50 and 75 °C, the average ligand numbers increase from ~ 1.5 to 2 at pH of 6.3−7 and reaches values of ~2.8−3.2 at pH between 7 and 9. The maximum average ligand number of 3.2 at 75 °C and pH of 9, within experimental uncertainty, is unlikely to indicate the stabilization of a $Er(OH)_4^-$ species, which is in line with the lack of such species in previous work in alkaline solutions[21,22]. Overall, we conclude that the increase in average ligand numbers with temperature suggests a growing predominance of the $Er(OH)_2^+$ and $Er(OH)_3^0$ species over the $Er(OH)^{2+}$ species.

Comparison of our results with the 25 °C experimental data by Han and Gysi[1] indicates that the $Er(OH)^{2+}$, $Er(OH)_2^+$, and $Er(OH)_3^0$ species are also stable at lower temperature over a pH range of 7.2 to 9.2. Stepanchikova *et al.*[14,30] show that the average ligand numbers for Tm^{3+} are between ~1.0 and 2.5 from pH 7.2 to 9.5 at low ionic strength and 25 °C, suggesting that $Tm(OH)^{2+}$, $Tm(OH)_2^+$, and $Tm(OH)_3^0$ are the predominant species in near-neutral to alkaline solutions. These results are in close agreement with the average ligand numbers determined for the Er hydrolysis at 35 °C in our study. At lower pH of 6.8 to 7.4 and 30 °C in 1 mol/L NaCl

283 solutions, Ramírez-García *et al.*[10] calculated average OH^- ligand numbers for Er to range
284 between ~ 0.04 and 0.15, which indicates the predominance of the Er^{3+} species with a small
285 proportion of $Er(OH)^{2+}$ species at these experimental conditions.

286 Wood *et al.*[21] carried out a series of solubility studies for the solid $Nd(OH)_3$ to
287 investigate the aqueous Nd hydroxyl complexes at temperatures between 30 to 290 °C with
288 0.03 mol/kg NaTr solution. The results from their solubility study at pH 5.2 to 10 indicate that
289 the hydrolysis in their experiments is predominantly controlled by the Nd^{3+} and $Nd(OH)_3^0$ as
290 temperature increase from 30 to 100 °C. At temperatures of 250 and 290 °C, the Nd^{3+},
291 $Nd(OH)^{2+}$, and $Nd(OH)_3^0$ control the Nd hydrolysis at the pH above 3.2, and the other species
292 $Nd(OH)_2^+$ is sensitive to the ionic strength at 290 °C.
293

294 **4.4. Er hydrolysis constants (*β_n°) and comparison to literature data**

295 The Er hydrolysis constants were derived from the calculated average ligand numbers and pH
296 determined in the Er-bearing *m*CP-NaOH solutions according to eqn (4). The logarithmic
297 values of the hydrolysis constants ($\log^*\beta_1^\circ$ to $\log^*\beta_3^\circ$) for $Er(OH)^{2+}$, $Er(OH)_2^+$, and $Er(OH)_3^0$
298 are listed in Table 2 and compared to literature values and theoretical predictions between
299 25−75 °C in Fig. 5.

300 To our knowledge, the retrieved $\log^*\beta_n^\circ$ values from our study are the first experimental
301 data available for the hydrolysis constants of Er at temperatures above 25 °C. The experimental
302 data (Table 2) were fitted from 25−75 °C to the temperature dependent equation $\log^*\beta_n^o = A_0$
303 $+ A_1T + A_2/T$, with T in Kelvin. The fitted coefficients A_0–A_2 and R^2 values are listed in Table
304 3. A comparison of the hydrolysis constants for $Er(OH)^{2+}$ and $Er(OH)_2^+$ at 25 and 35 °C
305 indicates that the stability of these species does not display significant differences (Fig. 5). In
306 contrast, the $Er(OH)_3^0$ species is more stable at 35 °C. These results suggest that the $Er(OH)^{2+}$

and $Er(OH)_2^+$ are not temperature dependent between 25 and 35 °C and the $Er(OH)_3^0$ depends on temperature. With increased temperature, the hydrolysis constants increase considerably between 25 and 75 °C, i.e. ~2−3 orders of magnitude for $\log^*\beta_1^\circ$ and $\log^*\beta_3^\circ$, and ~ 1 order of magnitude for $\log^*\beta_2^\circ$, respectively (Table 2).

In Part I of our study, the Er hydrolysis constants derived at 25 °C are discussed in more detail.[1] Other experimental studies conducted above 25 °C (Table 4) include Nazarenko *et al.*[31] who report the first conditional Er hydrolysis constant ($\log^*\beta_1$, at high ionic strength) to have a value of −6.56 at 30 °C in 0.1 mol/L $NaClO_4$ solution; Ramírez-García *et al.*[10] determined a $\log^*\beta_1$ value of −8.16 at 30 °C in 1 mol/L NaCl solution; Klungness and Byrne[9] determined $\log^*\beta_1$ values of −7.42 and −7.11 at 40 and 55 °C in 0.7 mol/L $NaClO_4$ solution. Because most of the other experimental literature data[9,32–36] were retrieved at low temperature or at high ionic strength (Table 4), a comparison to the hydrolysis constants above 25 °C can only be made in Fig. 5 with the calculated extrapolations from the study by Haas *et al.*[17]. Table 5 lists the smoothed fitted hydrolysis constants $^*\beta_1^\circ$–$^*\beta_3^\circ$ derived in this study which are compared to the values derived from Haas *et al.*[17]. The latter display difference ranging between ~0.4 to 1.5 logarithmic units. Further comparison of the Er hydrolysis constants functions with temperature (Fig. 5) indicates that only $^*\beta_1^\circ$ is reproduced by the extrapolations but need to be shifted to higher $\log^*\beta_1^\circ$ to reproduce our experimentally derived values. In contrast, $\log^*\beta_2^\circ$ and $\log^*\beta_3^\circ$ derived from our study are distinctly different, i.e. in the lower temperature range (25-50 °C) the correlations tend to under predict and in the higher temperature range (50-75 °C) they over predict the Er hydrolysis constants. These observations are in line with a few other studies that report that the stability of the REE hydroxyl complexes are over predicted with respect to the REE^{3+} aqua ion in hydrothermal solutions, as summarized in the review by Migdisov *et al.*[5].

The Er hydrolysis constants in Fig. 5 were further fitted using the Van't Hoff equation ($\ln{}^{*}\beta_n^{\circ}=-\Delta H^{\circ}/RT+\Delta S^{\circ}/R$) assuming the standard enthalpy (ΔH°) and entropy (ΔS°) values are constant between 25 and 75 °C. The standard thermodynamic properties of the $Er(OH)^{2+}$, $Er(OH)_2^{+}$, and $Er(OH)_3^{0}$ species at reference temperature of 298.15 K and pressure of 1 bar are summarized in Table 6. These values are retrieved from linear fits of the natural logarithm of the Er hydrolysis constants ($\ln{}^{*}\beta_n^{\circ}$) vs. 1/T (in Kevin), and using the Van't Hoff equation.

4.5. Er hydroxyl speciation as function of pH and temperature

A series of HCl/NaOH titration and speciation simulations was carried out using the GEMS code package[24] to show effect of temperature on the Er hydroxyl species distribution as function of pH. The simulations were carried out using the hydrolysis constant functions derived in this study (Table 3) and the functions derived by Haas *et al.*[17]. The latter study is the only available internally consistent dataset for all of the REE hydroxyl species with theoretical extrapolation to elevated temperature based on the revised Helgeson-Kirkham-Flowers (HKF) semi-empirical equation of state.[37–40] The aqueous REE hydroxyl species derived from Haas *et al.*[17] and other REE aqua ions, for example REE^{3+}, from other studies [39,41] are included in the program SUPCRT92[42], which are collectively referred to here as Supcrt92 database.

Figs. 6A-C illustrate the calculated pH-mole % Er species diagrams using the hydrolysis constants values derived in this study between 35 and 75 °C and pH ~6 to 9.5. The stability of the Er^{3+} aqua ion vs. Er hydroxyl complexes shifts gradually to more acidic pH with increased temperature. The overall abundance of the $Er(OH)_2^{+}$ species is larger than the $Er(OH)^{2+}$ species between 35 to 50 °C, whereas at 75 °C both reach a similar mol % depending on pH. The $Er(OH)_3^{0}$ species predominates at a pH above 8.0−8.5 at 35−50 °C and a pH above 7 at 75 °C. Hence, the $Er(OH)_3^{0}$ species displays a wider pH predominance field with increased

temperature. This behavior is also in line with the potentiometric data by Wood *et al.*[21], which indicate that the $Nd(OH)_3^0$ species predominates at pH above ~8.5 at 30−50 °C and at pH above ~7.5 at 100 °C.

Figs. 6D-F shows the modeled Er hydroxyl speciation distribution diagrams using the thermodynamic properties of Er^{3+} and Er hydroxyl complexes from the Supcrt92 database. A major difference to our study is the predominance of the $Er(OH)_4^-$ species at alkaline conditions (pH > 7.5−9.5) from the correlations derived by Haas *et al.*[17]. The presence of this species has not been identified based on the average ligand numbers derived in our study (Fig. 4), neither has it been observed for the hydrolysis of light REE such as Nd in the study by Wood *et al.*[21]. Furthermore, the modeled stability of Er^{3+} is over predicted in this model at temperatures of 35−50 °C, and the stability of the $Er(OH)_2^+$ species is under predicted over the stability of the $ErOH^{2+}$ species. The $ErOH^{2+}$ species also appears at pH values about 0.5 higher in comparison to the model based on data derived from our study.

Conclusions

The temperature effect on the complexation of Er at near-neural to alkaline pH was investigated by using UV-Vis spectrophotometry to determine *in situ* pH and the hydrolysis of Er. Comparison of the measured pH by the potentiometric method and this combined UV-Vis/*m*CP method indicates a good agreement at pH of ~6.3 to 9.5 and a temperature up to 75 °C. Furthermore, this UV-Vis shows a high sensitivity in pH measurement in alkaline solutions at high temperature and is therefore an ideal *in situ* method for studying the hydrolysis of REE.

The average ligand number and hydrolysis constants derived in our study indicate that the $Er(OH)^{2+}$, $Er(OH)_2^+$, and $Er(OH)_3^0$ species predominate at the studied experimental conditions, and that there is no evidence for the stabilization of the $Er(OH)_4^-$ species at pH

379 above 9, even at a temperature as high as 75 °C. The hydrolysis constants ($\log^*\beta_n^\circ$, n=1 to 3)
380 for these three species increase from 25 to 75 °C, and the stabilization of the $Er(OH)_3^0$ species
381 at alkaline pH shows a similar behavior to the hydrolysis of Nd based on the potentiometric
382 study by Wood *et al.*[21]. A comparison of the $\log^*\beta_n^\circ$ temperature functions derived in this study
383 with the hydrolysis constants derived and extrapolated to elevated temperature by Haas *et al.*[17]
384 indicates significant discrepancies. Overall, the $\log^*\beta_1^\circ$ values in our study are higher, and the
385 $\log^*\beta_2^\circ$ and $\log^*\beta_3^\circ$ temperature functions display lower values in comparison to Haas *et al.*[17].
386 These important discrepancies highlight the need to revise existing temperature functions from
387 Haas *et al.*[17] for the hydrolysis constants of all of the other REE, which may present variable
388 degrees of inaccuracies but are still used by most geochemical modeling programs.
389 Experimental data are therefore need for deriving more accurate REE hydrolysis constants to
390 model REE speciation as a function of pH and temperature. This work is part a comprehensive
391 and ongoing research effort to generate an internally consistent thermodynamic dataset for the
392 REE, which will be implemented in the MINES thermodynamic database[23].

393

394 **AUTHOR INFORMATION**

395 **Corresponding author**

396 **alexander.gysi@nmt.edu (A.P. Gysi)**

397

398 **Author contributions**

399 Hannah Juan Han: writing – original draft, methodology, formal analysis, investigation,
400 conceptualization, data curation. Alexander Gysi: writing – review & editing, validation,
401 supervision, resources, funding acquisition, data curation, conceptualization.

402

Data availability

The data published in this contribution are available as ESI submitted with the manuscript and in the Mendeley Data repository under doi: 10.17632/cjbczy723b.1

Conflicts of interest

There are no conflicts to declare.

ACKNOWLEDGMENTS

This work was supported by the U.S. Department of Energy, Office of Science, Office of Basic Energy Sciences, Geosciences program under Award Number DE-SC0021106 to AG. We are grateful to the Analytical Chemistry Laboratory at New Mexico Bureau of Geology for providing the ICP-OES. We would like to thank B. Frey and D. Baca for assistance on the ICP-OES instrument.

418 **References**

1 H. J. Han and A. P. Gysi, *Dalton Trans.*, 2024, **53**, 13129–13141.

2 A. P. Gysi and A. E. Williams-Jones, *Geochim. Cosmochim. Acta*, 2013, **122**, 324–352.

3 A. P. Gysi, A. E. Williams-Jones and P. Collins, *Econ. Geol.*, 2016, **111**, 1241–1276.

4 B. F. Walter, R. J. Giebel, M. Steele-MacInnis, M. A. W. Marks, J. Kolb and G. Markl, *Earth-Sci. Rev.*, 2021, **215**, 103509.

5 A. Migdisov, A. E. Williams-Jones, J. Brugger and F. A. Caporuscio, *Chem. Geol.*, 2016, **439**, 13–42.

6 M. Louvel, B. Etschmann, Q. Guan, D. Testemale and J. Brugger, *Nat. Commun.*, 2022, **13**, 1456.

7 H. Nisbet, A. A. Migdisov, V. Goncharov, V. van Hinsberg, A. E. Williams-Jones, H. Xu and X. Guo, *Chem. Geol.*, 2022, **611**, 121122.

8 L. G. Rodenas and S. J. Liberman, *Talanta*, 1991, **38**, 313–318.

9 G. D. Klungness and R. H. Byrne, *Polyhedron*, 2000, **19**, 99–107.

10 J. J. Ramírez-García, M. Solache-Ríos, M. Jiménez-Reyes and A. Rojas-Hernández, *J. Solut. Chem.*, 2003, **32**, 879–896.

11 J. J. Ramírez-García, M. Jiménez-Reyes, M. Solache-Ríos, E. Fernández-Ramírez, H. López-González and A. Rojas-Hernández, *J. Radioanal. Nucl. Chem.*, 2003, **257**, 299–303.

12 M. Jiménez-Reyes, M. Solache-Ríos and A. Rojas-Hernández, *J. Solut. Chem.*, 2006, **35**, 201–214.

13 M. A. Hernández-García, H. López-González and A. Rojas-Hernández, *Adv. Mater. Phys. Chem.*, 2015, **05**, 161.

14 S. A. Stepanchikova and R. P. Biteikina, *Russ. J. Coord. Chem. Khimiya*, 2011, **37**, 64–71.

15 S. A. Stepanchikova, R. P. Biteikina and G. P. Shironosova, *Russ. Geol. Geophys.*, 2014, **55**, 941–944.

16 S. A. Wood, *Chem. Geol.*, 1990, **82**, 159–186.

17 J. R. Haas, E. L. Shock and D. C. Sassani, *Geochim. Cosmochim. Acta*, 1995, **59**, 4329–4350.

18 P. L. Brown and C. Ekberg, *Hydrolysis of Metal Ions*, John Wiley & Sons, 2016.

19 J. Schijf and R. H. Byrne, *Chem. Geol.*, 2021, **584**, 120479.

20 Ç. İçhedef, T. Şişmanoğlu and S. Teksöz, *J. Solut. Chem.*, 2018, **47**, 220–230.

21 S. A. Wood, D. A. Palmer, D. J. Wesolowski and Pascale. Benezeth, *Spec. Publ. Geochem. Soc.*, 2002, **7**, 229–256.

22 N. Jordan, T. Thoenen, K. Spahiu, J. Kelling, S. Starke and V. Brendler, *Coord. Chem. Rev.*, 2024, **510**, 215702.

23 A. P. Gysi, N. C. Hurtig, R. Pan, G. D. Miron and D. A. Kulik, MINES Thermodynamic Database, *NM Bur. Geol. Min. Res.*, **version 23**, https://doi.org/10.58799/mines-tdb

24 D. A. Kulik, T. Wagner, S. V. Dmytrieva, G. Kosakowski, F. F. Hingerl, K. V. Chudnenko and U. R. Berner, *Comput. Geosci.*, 2013, **17**, 1–24.

25 G. D. Miron, T. Wagner, D. A. Kulik and C. A. Heinrich, *Geochim. Cosmochim. Acta*, 2016, **187**, 41–78.

26 S. A. Stepanchikova and G. I. Galay, *Russ. J. Phys. Chem. A*, 2017, **91**, 70–75.

27 A. Pietropaolo, C. Cozza, Z. Zhang and T. Nakano, *Liq. Cryst.*, 2018, **45**, 2048–2053.

28 G. Schwarzenbach and H. Flaschka in *Complexometric Titrations*, Methuen, London, 2nd English edn, 1969.

29 X. Liu, M. C. Patsavas and R. H. Byrne, *Environ. Sci. Technol.*, 2011, **45**, 4862–4868.

30 S. A. Stepanchikova, R. P. Biteykina and A. A. Sava, *Open J. Inorg. Chem.*, 2013, **03**, 42–47.

31 V. A. Nazarenko, V. P. Antonovich and E. M. Nevskaya, *Metal ions hydrolysis in dilute solutions*, Atomizdat, Moscow, 1979.

32 J. Kragten and L. G. Decnop-Weever, *Talanta*, 1983, **30**, 131–133.

33 U. K. Frolova, V. N. Kumok and V. V. Serebrennikov, *Khim Khim Tekhnol*, 1966, **9**, 176–179.

34 C. F. Baes and R. E. Mesmer in *The hydrolysis of cations*, Wiley, New York, 1976.

35 R. Guillaumont, B. Desire and M. Galin, *Radiochem. Radioanal. Lett.*, 1971, **8**, 189–197.

36 Y. Y. Yakubovich and V. G. Alekseev, *Russ. J. Inorg. Chem.*, 2012, **57**, 911–915.

37 H. C. Helgeson, D. H. Kirkham and G. C. Flowers, *Am. J. Sci.*, 1981, **281**, 1249.

38 J. C. Tanger and H. C. Helgeson, *Am. J. Sci.*, 1988, **288**, 19–98.

39 E. L. Shock and H. C. Helgeson, *Geochim. Cosmochim. Acta*, 1988, **52**, 2009–2036.

40 E. L. Shock, E. H. Oelkers, J. W. Johnson, D. A. Sverjensky and H. C. Helgeson, *J. Chem. Soc. Faraday Trans.*, 1992, **88**, 803–826.

41 E. L. Shock, D. C. Sassani, M. Willis and D. A. Sverjensky, *Geochim. Cosmochim. Acta*, 1997, **61**, 907–950.

42 J. W. Johnson, E. H. Oelkers and H. C. Helgeson, *Comput. Geosci.*, 1992, **18**, 899–947.

Data availability

The data published in this contribution are available as ESI submitted with the manuscript and in the Mendeley Data repository under doi: 10.17632/cjbczy723b.1

1 **Figures**

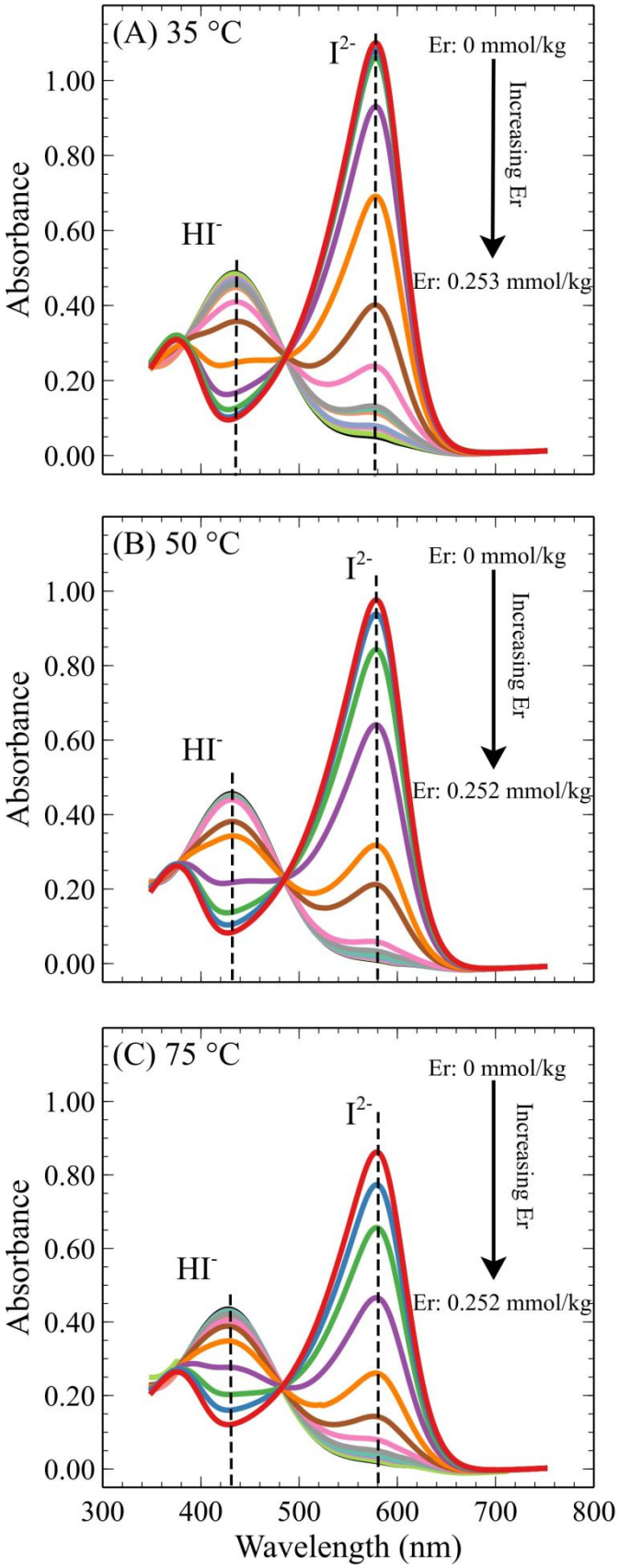

2 **Figure 1**. UV-Vis spectra of 0.030 mmol/kg *m*CP in 0.445 mmol/kg NaOH with addition of varying
3 Er concentrations ranging from 0.000 to 0.253 mmol/kg at (A) 35 °C, (B) 50 °C, and (C) 75 °C.

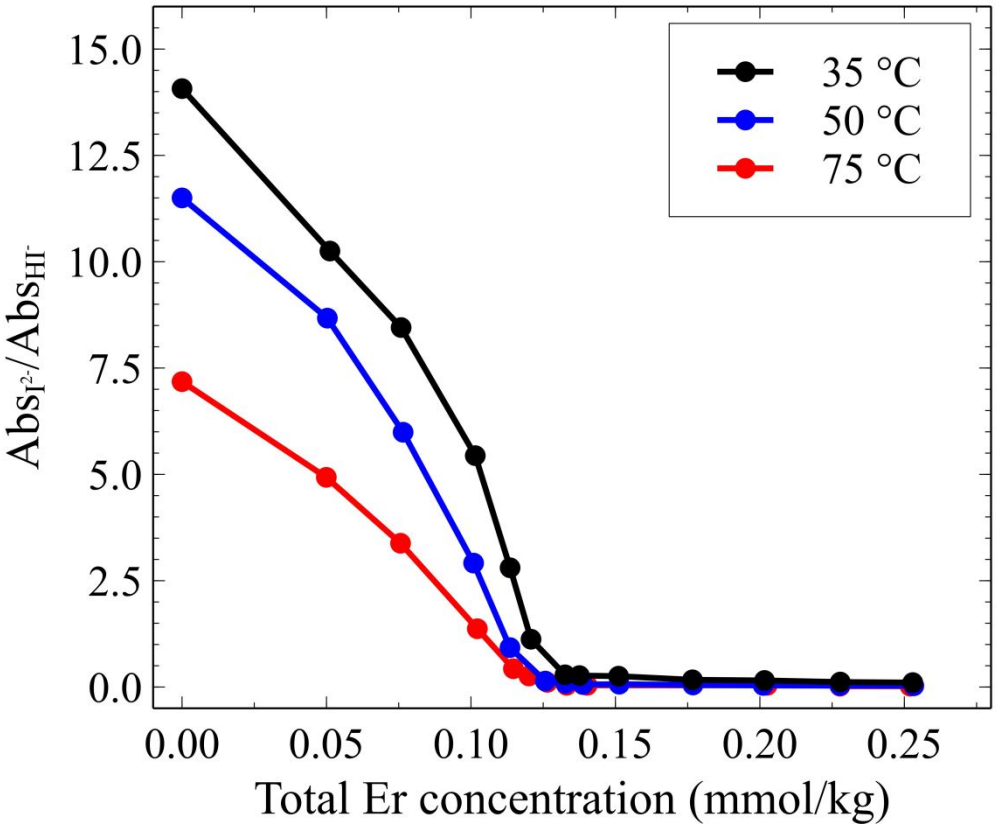

Figure 2. *m*CP absorbance intensity ratio (*R*, Abs_{I2-}/Abs_{HI-}) of its basic (I^{2-}) to its acidic form (HI^-) at their maximum wavelengths as a function varying Er concentrations at temperatures of 35−75 °C. Uncertainties are smaller than the symbol sizes.

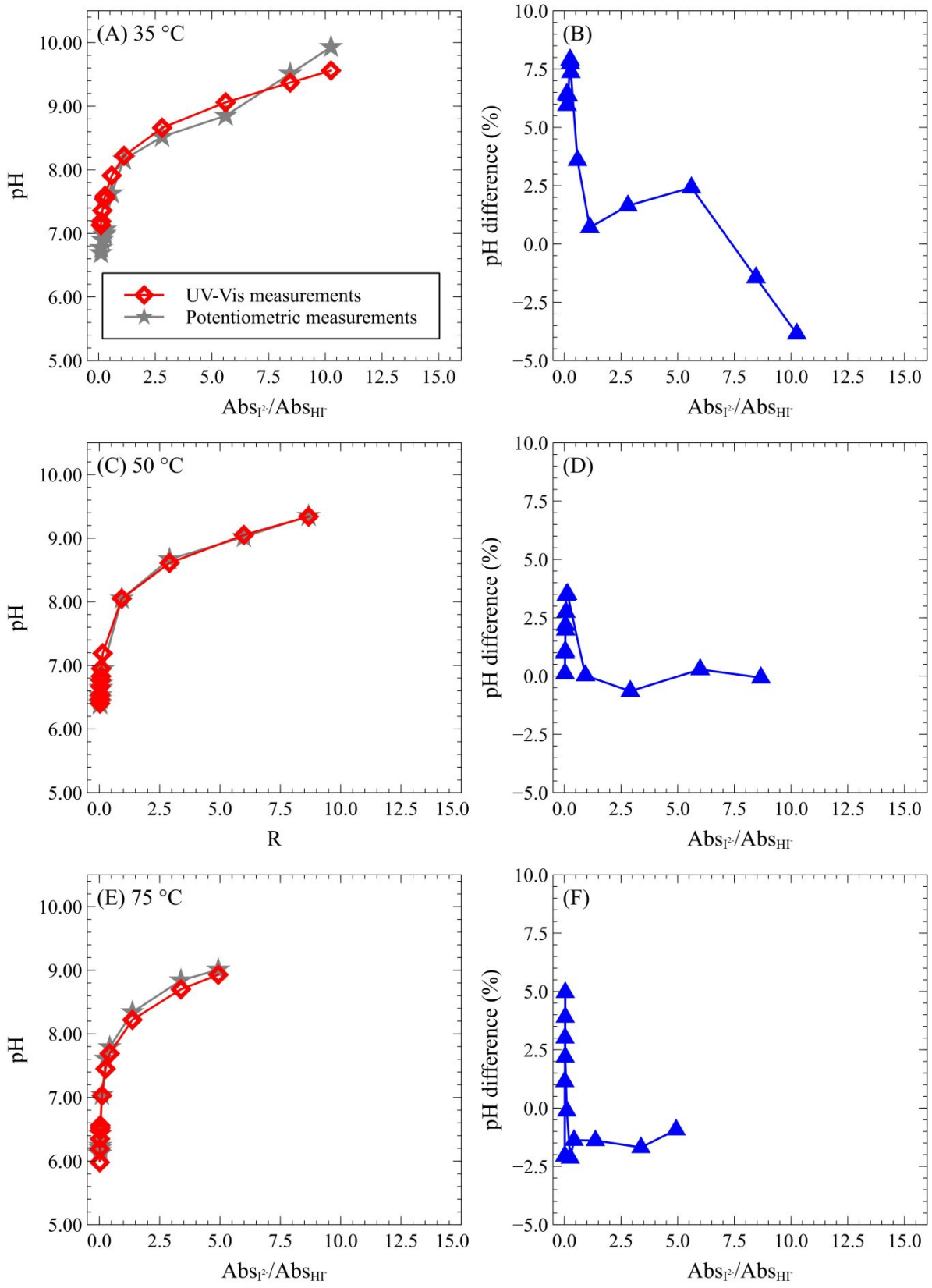

Figure 3. Comparison between measured pH by potentiometry and UV-Vis/*m*CP method (A,C,E) and percent deviation (B,D,F) between both methods as a function of the *m*CP absorbance intensity ratio (*R*, Abs_{I2-}/Abs_{HI-}) of its basic (I^{2-}) to its acidic (HI^-) forms at 35−75 °C. Uncertainties are smaller than the symbol sizes.

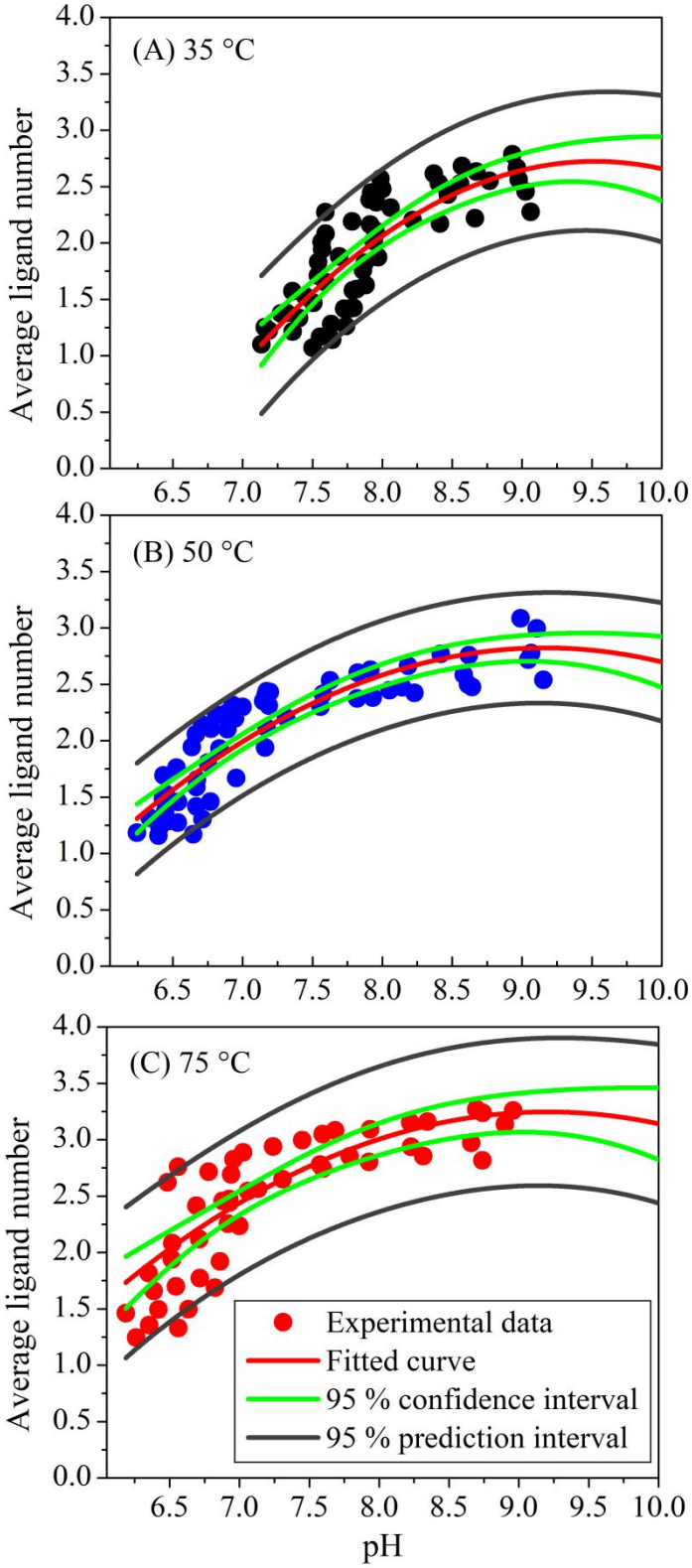

Figure 4. Calculated average number of OH^- ligands coordinated to Er^{3+} and pH determined by UV-Vis in experimental *m*CP-NaOH solutions with varying Er concentrations (0 to ~0.253 mmol/kg Er) and pH values between ~6.3 to 9.0 at (A) 35 °C, (B) 50 °C, and (C) 75 °C. Also shown are the fits to the experimental data, their 95% confidence and prediction interval. The experimental data and fitted equations and coefficients are listed in Table S1 and Table 1, respectively.

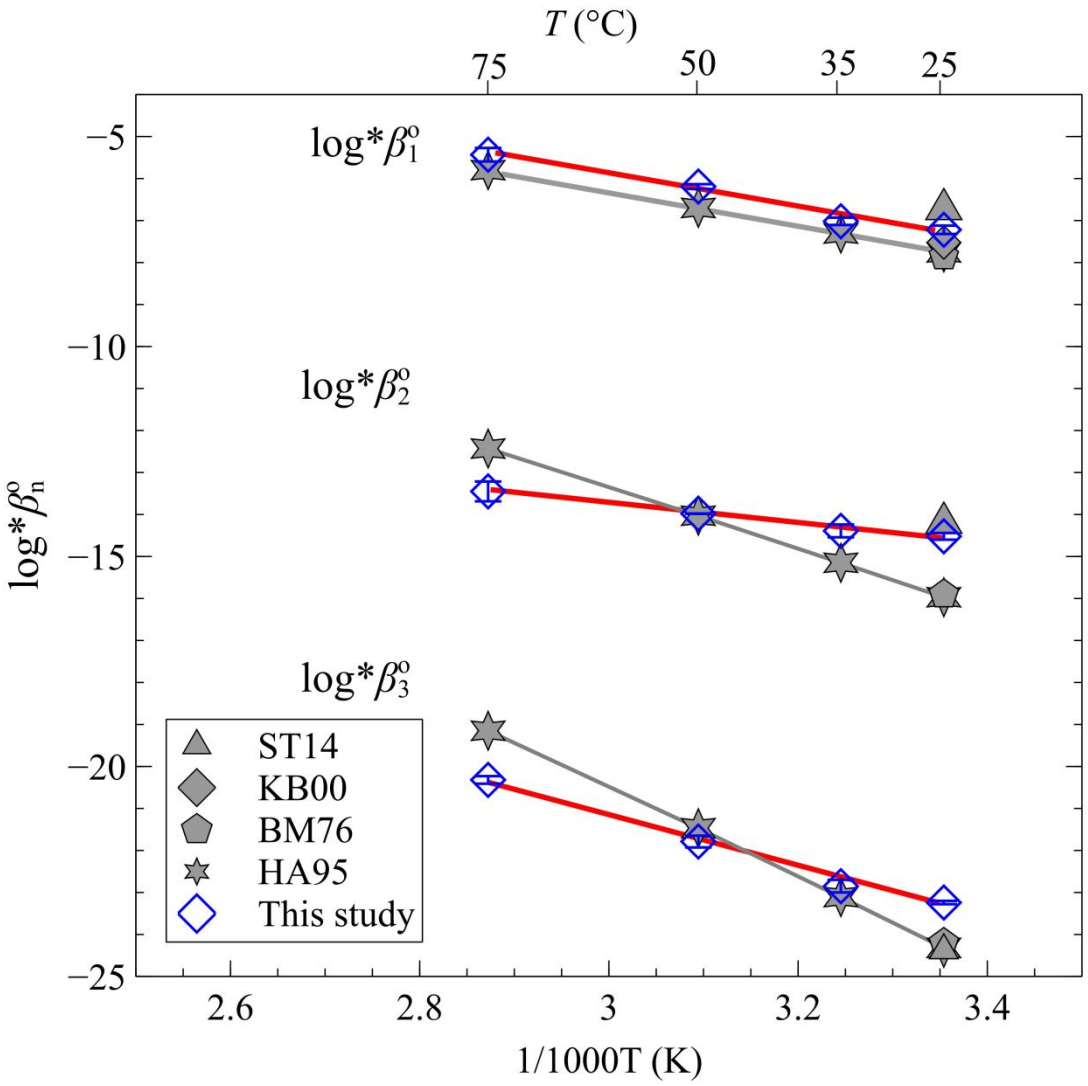

Figure 5. Hydrolysis constant ($\log^*\beta_n^\circ$, n = 1 to 3) of Er ($REE^{3+} + nH_2O = REE(OH)_n^{3-n} + nH^+$, with n=1 to 3) as a function of temperature between 25 and 75 °C showing a comparison of the experimental data from this study (Table 2) and by Han and Gysi[1] with the extrapolations from Haas *et al.*[17]. The regressed coefficients for fits to our data are listed in Table 3. Additional references include (Table 4): [ST14][15]; [BM76][34]; [KB00][9]; [HA95][17].

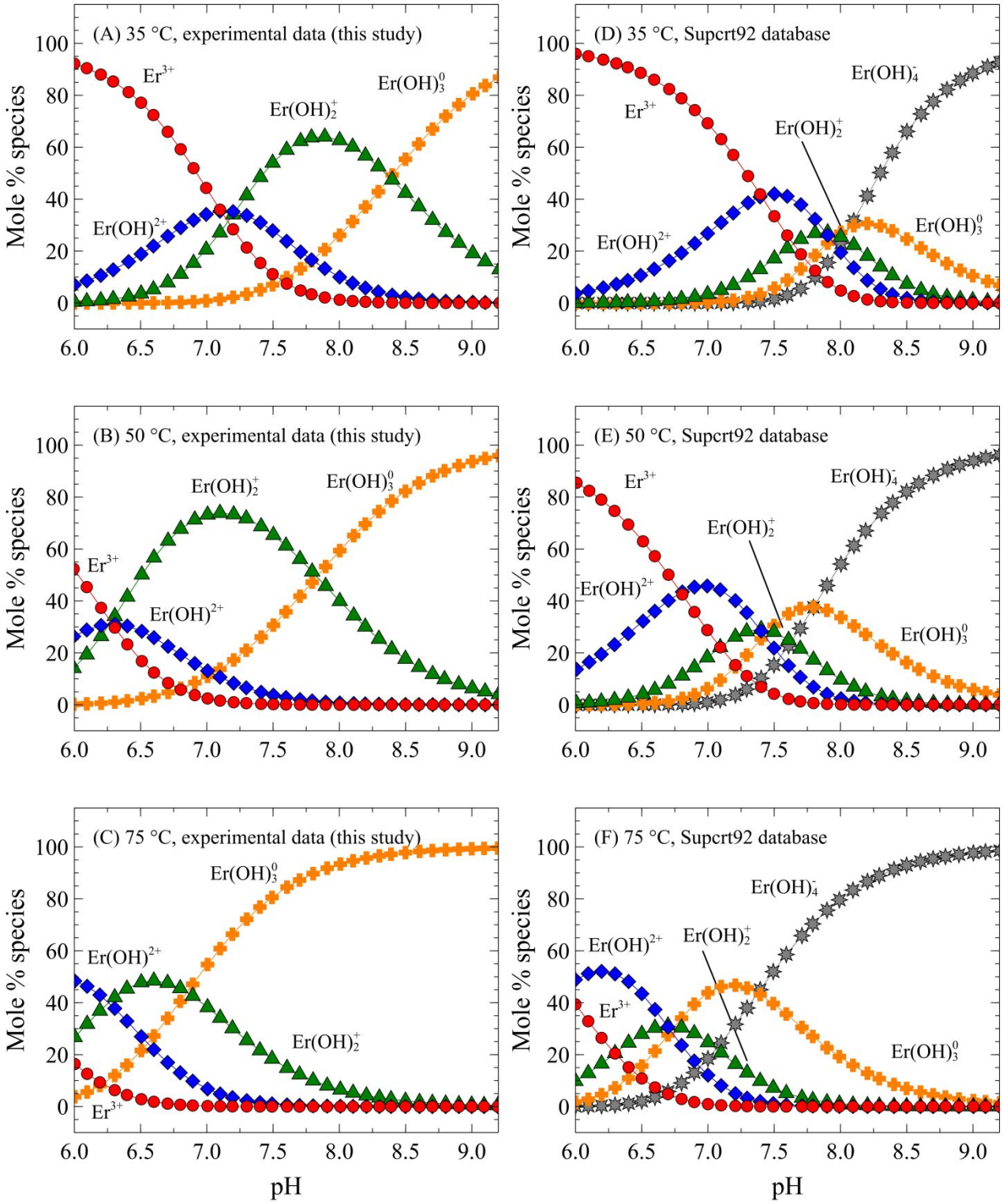

Figure 6. Speciation diagram of the aqueous Er^{3+} and Er hydroxyl complexes system at pH of 6 to 9.2 and temperature of 35 to 75 ℃. Diagrams were calculated using GEMS code package[24] and HCl/NaOH titration model using the Er hydrolysis constants derived in this study and by Han and Gysi[1] (A-C) derived in this study and (D-F) predicted using the Supcrt92[17,37–42] database. Thermodynamic properties for other species were taken from the MINE thermodynamic database[23].

Table 1. Regressed fits of the average ligand number of Er ($\bar{n}$) determined at 35−75 ℃ as function of pH between 6.3 and 9.5. The the experimental data for the determination of average ligand number at 35−75 ℃ are listed in Table S1.

T (°C)	Fitted equation: $\bar{n}=ax^2+bx+c$			R^2	RSME
	a	b	c		
35	-0.285	5.431	-23.13	0.6811	0.2917
50	-0.178	3.254	-12.09	0.7960	0.2370
75	-0.166	3.056	-10.82	0.6539	0.3111

Table 2. The logarithmic values of the Er hydrolysis constants ($\log^*\beta_n^o$, $Er^{3+} + nH_2O = Er(OH)_n^{3-n} + nH^+$, n=1 to 3) determined in this study at 35−75 ℃ using UV-Vis spectrophotometry. The standard deviation of the mean (1σ) is based on replicate experiments (Table S1).

T (°C)	$\log^*\beta_1^o$	1σ	$\log^*\beta_2^o$	1σ	$\log^*\beta_3^o$	1σ
25[a]	-7.22[a]	0.10[a]	-14.52[a]	0.08[a]	-23.24[a]	0.04[a]
35	-7.02	0.09	-14.39	0.15	-22.85	0.15
50	-6.19	0.06	-13.98	0.01	-21.79	0.14
75	-5.43	0.16	-13.45	0.24	-20.32	0.09

[a]Derived by Han and Gysi[1] at 25 ℃ using UV-Vis spectrophotometry.

Table 3. Regressed coefficients for the function expressing the logarithm of the hydrolysis constants ($\log^*\beta_n^o$, $Er^{3+} + nH_2O = Er(OH)_n^{3-n} + nH^+$, n=1 to 3) as a function of temperature from 25 to 75 °C. These regressions are generated using the experimental data from Table 2. The regressed function used is: $\log^*\beta_n^o = A_0 + A_1T + A_2/T$, with T in Kelvin.

	A_0	$A_1 \times 10^3$	A_2	R^2
(β_1)	1.631	6.4374	-3231.7	0.982
(β_2)	-28.22	33.024	1142.0	0.993
(β_3)	-63.27	94.034	3560.4	0.996

Table 4. Compilation of available literature data for the Er hydrolysis constants log*β_1^o to log*β_3^o.

Author	Method	T (°C)	Ionic strength and medium[a]	log*β_1[b]	log*β_2[b]	log*β_3[b]
Kragten and Decnop-Weever [32]	Solubility	21.5	1 M $NaClO_4$	−6.3	−14.5	−23.1
Frolova et al.[33]	Potentiometry	25	0.3 M $NaClO_4$	−7.99		
Baes and Mesmer[34]	Empirical fits and data compilation	25	infinite dilution	−7.85	−15.90	−24.20
Guillaumont *et al.*[35]	Solvent extraction	25	0.1 M $HClO_4$/$LiClO_4$	−5.5		
Klungness and Byrne[9]	Potentiometry	25	infinite dilution	−7.52		
Yakubovich and Alekseev[36]	Potentiometry	25	0.1 M KNO_3	−7.63	−16.15	−22.23
Stepanchikova *et al.*[15]	Spectrophotometry	25	0.0005 M	−6.73	−14.20	−24.38
Han and Gysi[1]	Spectrophotometry	25	0.001 M	−7.22	−14.52	−23.24
Nazarenko *et al.*[31]	Empirical fits and data compilation	30	0.1 M $NaClO_4$	−6.56		
Ramírez-García *et al.*[10]	Potentiometry	30	1 M NaCl	−8.16		
Klungness and Byrne[9]	Potentiometry	40	0.7 M $NaClO_4$	−7.42		
Klungness and Byrne[9]	Potentiometry	55	0.7 M $NaClO_4$	−7.11		

[a]Concentration units in M is mol/L; m is mol/kg. [b]Note that the symbol (°) was omitted because a few studies at high ionic strength report a conditional equilibrium constants not extrapolated to infinite dilution.

Table 5. Comparison between the Er hydrolysis constants derived from the smoothed temperature function from this study (Table 3) and the values retrieved from the thermodynamic correlations derived by Haas *et al.*[17] [HA95]. Δ represent the differences between our study and [HA95].

T (°C)	log*β_1^o (this study)	log*β_1^o [HA95]	Δ	log*β_2^o (this study)	log*β_2^o [HA95]	Δ	log*β_3^o (this study)	log*β_3^o [HA95]	Δ
25	-7.3	-7.8	0.5	-14.5	-16.0	1.5	-23.3	-24.3	1.0
35	-6.9	-7.3	0.4	-14.3	-15.2	0.9	-22.7	-23.1	0.4
50	-6.3	-6.7	0.4	-14.0	-14.0	0.0	-21.9	-21.5	-0.4
75	-5.4	-5.8	0.4	-13.4	-12.4	-1.0	-20.3	-19.2	-1.1

Table 6. Standard thermodynamic properties of Er hydroxyl complexes (at reference temperature of 298.15 K and pressure of 1 bar) and fits of natural logarithm of Er hydrolysis constants derived in this study and 1/T (in Kevin) at 25 and 75 °C.

Species	$\Delta_r G^\circ_{298}$	$\Delta_r H^\circ_{298}$	$\Delta_r S^\circ_{298}$	$\ln{}^*\beta_n^\circ = a/T + b$			*T* range
	kJ/mol	kJ/mol	J/mol/K	a	b	R^2	°C
$Er(OH)^{2+}$	41.2	74.3	110.9	-8984.82	13.34	0.98	25−75
$Er(OH)_2^+$	82.9	43.7	-131.5	-5289.01	-15.82	0.99	25−75
$Er(OH)_3^0$	132.7	118.5	-47.3	-14349.57	-5.69	0.99	25−75